Master's Thesis,
PHYM01
May 2, 2018

Thermodynamics of a Two-Qubit Absorption-Driven Heat Pump

LUND
UNIVERSITY

Gustav Seemann

Division of Mathematical Physics, Department of Physics, Lund University

Supervised by Peter Samuelsson
Co-supervised by Fredrik Brange

Abstract

Quantum thermal machines, a sub-field of quantum thermodynamics, are actively studied with the aim to understand the connection between quantum mechanics and thermodynamics. In this work, qubits are used as the active medium in an absorption driven heat pump. The dynamics of this thermal machine are computationally simulated by treating the qubits as an open quantum system interacting with three bosonic heat baths. Some thermodynamic bounds for the system parameters are derived and used in order to define a refrigerating regime for the system.

Acknowledgements

I would like to thank Peter Samuelsson and Fredrik Brange for the supervision of my thesis work. I have appreciated your support and pedagogical explanations throughout the project. I would also like to thank everyone else at the division of mathematical physics for the hospitality and for providing a pleasant working environment. My family also deserves the greatest gratitude for supporting me every day, through thick and thin. Without you I would never have reached this point of completing a master's thesis in engineering. Thank you!

Contents

1 Introduction

The study of quantum thermodynamics, and more specifically quantum thermal machines, is an active field of research. The aim is to extend the field of thermodynamics, to include descriptions of non-equilibrium effects and small ensemble sizes. Experimentalists have gained access to, and control over, quantum systems and implementation of nano-scale components and devices have become a reality. This presents a possibility and a potential need to work with thermodynamic applications at the same scale. To develop an understanding of the system studied in this thesis elements from different branches of physics have to be considered. Quantum information theory is closely linked to thermodynamics, and emphasized through the use of qubits. The theory of open quantum systems is needed in order to arrive at an equation of motion specific for the heat pump considered. The performance of the thermal machine is understood and evaluated through a thermodynamic point of view.

2 Theory

2.1 Quantum Information

The field of quantum information is a relatively new branch of science, developed in order to explore information theory and information processing supported by quantum mechanical systems. In [8] it is described how classical information theory in a way has parted from physics in the sense that the concept of information can be treated independent of physical support. It turns out that different entropy measures are sufficient to quantify outcomes in information theory. Information entropy may characterize the probability distributions of outcomes, not bothering with the physical content of the events. For example, a fair coin toss may result in either heads or tails, i.e. two discrete and equally probable events. The entropy of the coin toss is defined to be $\log_2 2 = 1$ bit. This entropy would be the same for any system producing an equally weighed binary outcome, regardless of the physical support.

"*But as it turned out, not all information was created equal.*"
Goold, J. p.2 [8]

When experimentalists gained access to individual quantum systems, predicted quantum phenomena could be tested. At the heart of these discoveries lie non-local correlations between quantum systems, according to [5] and [13].

Classical physics relies on the assumption of locality, that is the premise that a measurement at one point in space would not affect the results of a measurement at another point in space. Suddenly there was a need to revert to physics in order to explain such anomalies.

These non-local correlations, generally called entanglement, appear solely in quantum mechanics. As it turns out, several purely quantum mechanical phenomena appear related to information theory, e.g. the no-cloning theorem, quantum teleportation, quantum key distribution and quantum algorithms that would outdo their classical counterparts when implemented.

2.1.1 Qubits

In classical information science the bit constitutes the elementary building block. A bit can be realized by any two-state device and can at any given time hold only one of two values. In processors, for example, transistors are used to represent bits where they, depending on the applied gate voltage, can be either on or off. These two values are most commonly denoted as 0 and 1. In the transition to quantum information science the concept of bits had to be revisited due to quantum superposition. The quantum counterpart of the bit is called a qubit, a portmanteau of "quantum bit".

"*Associated to any isolated physical system is a complex vector space with inner product (that is, a Hilbert space) known as the state space of the system. The system is completely described by its state vector, which is a unit vector in the system's state space*"
Nielsen, M.A. and Chuang, I.L. p.80 [13]

The following is mainly based on the information found in [13]. A qubit can be represented by a simple quantum system having a two-dimensional state space. By convention, here in Dirac notation, $|0\rangle$ and $|1\rangle$ are chosen as an orthonormal base for this space. Quantum superposition allows the system to be in a state that is a linear combination of the two pure states, $|0\rangle$ and $|1\rangle$, as

$$|\psi\rangle = a\,|0\rangle + b\,|1\rangle\,, \tag{1}$$

where $\{a,b\} \in \mathbb{C}$. Additionally, for $|\psi\rangle$ to be a unit vector the normalization criterion $\langle\psi|\psi\rangle = 1$ has to be fulfilled.

Equation 1 indicates that the state, $|\psi\rangle$, is a continuous variable - that qubits can represent an infinite amount of states. This seems to contradict the statement that the qubit is the fundamental unit of quantum information. However, the resolution of measurements on qubits is limited to only yield one

bit of information. The measurement itself causes the superposition of the state to collapse into either $|0\rangle$ or $|1\rangle$. A large number of measurements on an equally large ensemble of identically prepared qubits would be able to resolve the state prior to measurement as the probabilities of the outcomes are $|a^2|$ and $|b^2|$, for $|0\rangle$ and $|1\rangle$ respectively. As usual for probabilities $|a|^2 + |b|^2 = 1$ always applies, being equivalent to the normalization criterion. pp.13-16 [13]

A mathematical description of a qubit is of course important, but to actually implement quantum circuits a suitable physical representation has to be found. In ch.7 of [13], several different plausible physical supports are presented, e.g. polarization of a photon, an atom in an electromagnetic cavity, trapped ions, nuclear spins resolved by nuclear magnetic resonance (NMR), etc. However, there are also several criteria that a physical representation has to meet for it to be promising for implementations. The system has to maintain its quantum character, be able to robustly hold information, the evolution of the state (through unitary transformations) must be controllable, one has to be able to prepare the system in a desired initial reference state and, of course, the system has to be accessible to measurements. These criteria, or constraints, imply different strengths and weaknesses to the examples of physical representations mentioned above.

2.1.2 Bloch Sphere Representation

The mathematical definition of qubits is a bit cumbersome to get an intuitive grasp on, but fortunately there is a way to geometrically illustrate the state-space of a qubit ($\mathbb{C}^2$). This representation also makes it feasible to picture the evolution of a qubit's state vector through different linear operations. To approach this representation the state can be expressed as

$$|\psi\rangle = e^{i\gamma}\left(\cos\left(\frac{\theta}{2}\right)|0\rangle + e^{i\phi}\sin\left(\frac{\theta}{2}\right)|1\rangle\right), \tag{2}$$

$$\text{with } \{\theta,\, \phi,\, \gamma\} \in \mathbb{R},$$
$$0 \leq \theta \leq \pi \text{ and } 0 \leq \phi \leq 2\pi,$$

again fulfilling the normalization condition $\langle\psi|\psi\rangle = 1$.

To further simplify the expression above it is noted that the global phase of a state, $e^{i\gamma}$, does not affect the outcome of a measurement. This can be verified by showing that the measurement outcome m using a measurement operator $\hat{M}_m$ on the state $|\psi\rangle$, is not affected by the phase: $\langle\psi|e^{-i\gamma}\hat{M}_m^\dagger\hat{M}_m e^{i\gamma}|\psi\rangle = \langle\psi|\hat{M}_m^\dagger\hat{M}_m|\psi\rangle$. Because of this the global phase can be factored out, letting

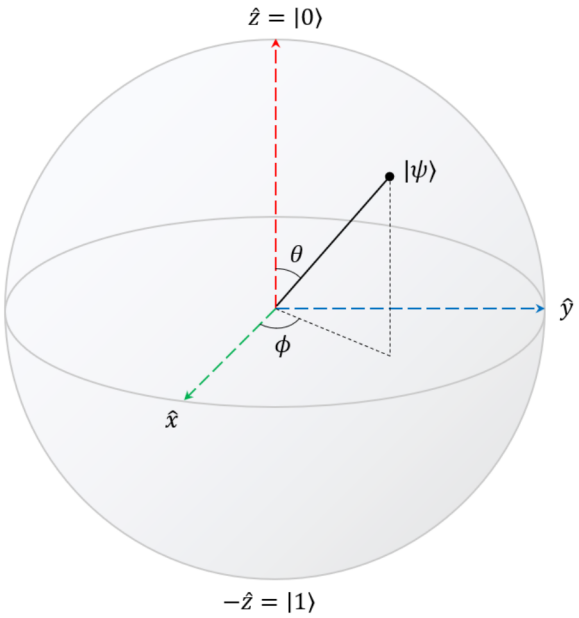

Figure 1: The Bloch Sphere with $|0\rangle$ and $|1\rangle$ as an orthonormal basis. $|\psi\rangle$ is an arbitrary state of the system.

us only consider the relative phase between the coefficients. Choosing the phase of $|0\rangle$ to be real and positive the state can be written as

$$|\psi\rangle = \cos\left(\frac{\theta}{2}\right)|0\rangle + e^{i\phi}\sin\left(\frac{\theta}{2}\right)|1\rangle\,. \tag{3}$$

This state can now be represented using spherical coordinates (r, θ, ϕ), with r as the radial distance, θ as the polar angle and ϕ as the azimuthal angle. This is illustrated in Fig. 1. Pure states will always move along the surface of the Bloch sphere, through unitary transformations, as the length of the vector equals one ($r = 1$). Both [13] and [1] provide a good overview of the Bloch Sphere representation of a qubit.

2.2 Quantum Mechanics

In order to describe the evolution of general quantum systems some concepts have to be clarified. How can the time evolution of a system be properly described? What are the mathematical building blocks of the Hilbert space, and what operators govern transformations on this space?

2.2.1 Constructing the Hilbert Space

Transformations within a Hilbert space of dimension $\mathbb{C}^n$ constitute a Lie group SU(n), which means that the group of transformations is continuous. Again referring to the Bloch sphere it can be seen as the fact that the coefficients a and b in Eq. 1 can take any values as long as $|a|^2 + |b|^2 = 1$. A more general section about operators is found in Appendix A. The Hamiltonians acting on a two dimensional state space belong to the special unitary group of degree 2, SU(2). This group is defined as

$$SU(2) = \left\{ \begin{bmatrix} \alpha & \beta \\ -\bar{\beta} & \bar{\alpha} \end{bmatrix} \;\middle|\; \alpha,\, \beta \in \mathbb{C}\ ,\ |\alpha|^2 + |\beta|^2 = 1 \right\}. \tag{4}$$

As the name of the group indicates all matrices in the expression above are unitary, which is readily confirmed by

$$U(\alpha,\beta)^\dagger U(\alpha,\beta) = \begin{bmatrix} \bar{\alpha} & -\beta \\ \bar{\beta} & \alpha \end{bmatrix} \begin{bmatrix} \alpha & \beta \\ -\bar{\beta} & \bar{\alpha} \end{bmatrix} = \mathbb{1}_2. \tag{5}$$

Topologically, SU(2) is the unit sphere inside $\mathbb{C}^2$, cf. the Bloch sphere. A brief overview of e.g. SU(2) is given in sec.3.3 in [15], while a more detailed insight is provided by ch.16 in [9].

As it turns out the Pauli matrices:

$$\begin{aligned} \sigma_1 = \sigma_x &= \begin{bmatrix} 0 & 1 \\ 1 & 0 \end{bmatrix}, \\ \sigma_2 = \sigma_y &= \begin{bmatrix} 0 & -i \\ i & 0 \end{bmatrix}, \\ \sigma_3 = \sigma_z &= \begin{bmatrix} 1 & 0 \\ 0 & -1 \end{bmatrix} \end{aligned} \tag{6}$$

are suitable for spanning the corresponding Lie algebra $\mathfrak{su}(2)$. This means that any Hamiltonian operator acting on a $\mathbb{C}^2$ Hilbert space can be represented as a linear combination of the Pauli matrices.

For the case of two qubits, the state space has to be expanded to $\mathbb{C}^4$. It is shown in [7] how this can readily be done by using the extended Pauli matrices, i.e. $\sigma_{1,2,3}$ together with the 2x2 identity matrix

$$\sigma_0 = \mathbb{1}_2 = \begin{bmatrix} 1 & 0 \\ 0 & 1 \end{bmatrix}. \tag{7}$$

The tensor products

$$D_{ij} = \sigma_i \otimes \sigma_j \text{ for } i,j \in \{0, 1, 2, 3\} \tag{8}$$

generate 16 4x4 hermitian matrices.

i \ j	0	1	2	3
0	$\mathbb{1}_2 \otimes \mathbb{1}_2 = \mathbb{1}_4$	$\begin{bmatrix} 0 & 1 & 0 & 0 \\ 1 & 0 & 0 & 0 \\ 0 & 0 & 0 & 1 \\ 0 & 0 & 1 & 0 \end{bmatrix}$	$\begin{bmatrix} 0 & -i & 0 & 0 \\ i & 0 & 0 & 0 \\ 0 & 0 & 0 & -i \\ 0 & 0 & i & 0 \end{bmatrix}$	$\begin{bmatrix} 1 & 0 & 0 & 0 \\ 0 & -1 & 0 & 0 \\ 0 & 0 & 1 & 0 \\ 0 & 0 & 0 & -1 \end{bmatrix}$
1	$\begin{bmatrix} 0 & 0 & 1 & 0 \\ 0 & 0 & 0 & 1 \\ 1 & 0 & 0 & 0 \\ 0 & 1 & 0 & 0 \end{bmatrix}$	$\begin{bmatrix} 0 & 0 & 0 & 1 \\ 0 & 0 & 1 & 0 \\ 0 & 1 & 0 & 0 \\ 1 & 0 & 0 & 0 \end{bmatrix}$	$\begin{bmatrix} 0 & 0 & 0 & -i \\ 0 & 0 & i & 0 \\ 0 & -i & 0 & 0 \\ i & 0 & 0 & 0 \end{bmatrix}$	$\begin{bmatrix} 0 & 0 & 1 & 0 \\ 0 & 0 & 0 & -1 \\ 1 & 0 & 0 & 0 \\ 0 & -1 & 0 & 0 \end{bmatrix}$
2	$\begin{bmatrix} 0 & 0 & -i & 0 \\ 0 & 0 & 0 & -i \\ i & 0 & 0 & 0 \\ 0 & i & 0 & 0 \end{bmatrix}$	$\begin{bmatrix} 0 & 0 & 0 & -i \\ 0 & 0 & -i & 0 \\ 0 & i & 0 & 0 \\ i & 0 & 0 & 0 \end{bmatrix}$	$\begin{bmatrix} 0 & 0 & 0 & -1 \\ 0 & 0 & 1 & 0 \\ 0 & 1 & 0 & 0 \\ -1 & 0 & 0 & 0 \end{bmatrix}$	$\begin{bmatrix} 0 & 0 & -i & 0 \\ 0 & 0 & 0 & i \\ i & 0 & 0 & 0 \\ 0 & -i & 0 & 0 \end{bmatrix}$
3	$\begin{bmatrix} 1 & 0 & 0 & 0 \\ 0 & 1 & 0 & 0 \\ 0 & 0 & -1 & 0 \\ 0 & 0 & 0 & -1 \end{bmatrix}$	$\begin{bmatrix} 0 & 1 & 0 & 0 \\ 1 & 0 & 0 & 0 \\ 0 & 0 & 0 & -1 \\ 0 & 0 & -1 & 0 \end{bmatrix}$	$\begin{bmatrix} 0 & -i & 0 & 0 \\ i & 0 & 0 & 0 \\ 0 & 0 & 0 & i \\ 0 & 0 & -i & 0 \end{bmatrix}$	$\begin{bmatrix} 1 & 0 & 0 & 0 \\ 0 & -1 & 0 & 0 \\ 0 & 0 & -1 & 0 \\ 0 & 0 & 0 & 1 \end{bmatrix}$

Table 1: The 16 4x4 matrices given from Eq. 8, with i and j corresponding to the indexes of D_{ij} in the same equation. Except from D_{00}, they are generators of the $\mathfrak{su}(4)$ Lie algebra, why linear combinations of them can construct any Hamiltonian for a two qubit Hilbert space.

The tensor product as a mathematical tool will be described further on, in section 2.3.4. Short of the identity matrix $\mathbb{1}_4$, D_{00}, they constitute a generator set for the Lie algebra $\mathfrak{su}(4)$. Just as the Pauli matrices in the $\mathbb{C}^2$ case, it means that any Hamiltonian acting on a two qubit system can be represented as a linear combination of the matrices in table 1.

2.2.2 Ladder Operators

The ladder operators for a qubit can be constructed through linear combinations of the Pauli matrices in Eq. 6. The raising and lowering operators, σ^+ and σ^- respectively, moves the state from one eigenstate to the other. They are constructed according to

$$\sigma^+ = \frac{\sigma_x + i\sigma_y}{2} = \begin{bmatrix} 0 & 1 \\ 0 & 0 \end{bmatrix} \tag{9}$$

and

$$\sigma^- = \frac{\sigma_x - i\sigma_y}{2} = \begin{bmatrix} 0 & 0 \\ 1 & 0 \end{bmatrix} \tag{10}$$

For a two qubit system, in $\mathbb{C}^4$, the raising and lowering operators for each qubit can be constructed with the help of σ_0, as

$$\begin{aligned} \sigma_1^+ = \sigma^+ \otimes \sigma_0 = \begin{bmatrix} 0 & 0 & 1 & 0 \\ 0 & 0 & 0 & 1 \\ 0 & 0 & 0 & 0 \\ 0 & 0 & 0 & 0 \end{bmatrix} \qquad \sigma_1^- = \sigma^- \otimes \sigma_0 = \begin{bmatrix} 0 & 0 & 0 & 0 \\ 0 & 0 & 0 & 0 \\ 1 & 0 & 0 & 0 \\ 0 & 1 & 0 & 0 \end{bmatrix} \\ \sigma_2^+ = \sigma_0 \otimes \sigma^+ = \begin{bmatrix} 0 & 1 & 0 & 0 \\ 0 & 0 & 0 & 0 \\ 0 & 0 & 0 & 1 \\ 0 & 0 & 0 & 0 \end{bmatrix} \qquad \sigma_2^- = \sigma_0 \otimes \sigma^- = \begin{bmatrix} 0 & 0 & 0 & 0 \\ 1 & 0 & 0 & 0 \\ 0 & 0 & 0 & 0 \\ 0 & 0 & 1 & 0 \end{bmatrix} \end{aligned} \tag{11}$$

where the indices 1 and 2 indicate which qubit the operator is acting on.

2.3 Open Quantum Systems

"In contrast to the case of a closed systems [sic], the quantum dynamics of an open system cannot, in general, be represented in terms of a unitary time evolution. In many cases it turns out to be useful to formulate, instead, the dynamics of an open system by means of an appropriate equation of motion for its density matrix, a quantum master equation."
Breuer H.P. and Petruccione F. p.109 [3]

In real physical systems there is no such thing as a perfectly closed quantum system. The system in question will inevitably interact with adjacent systems, or an environment. In the end, the only system thought to be closed is the universe itself. However, to treat systems that big would be near impossible. If the interest lies only in the dynamics of a subsystem, just a fraction of the whole, this vast description might be superfluous. Because of this it is appropriate to instead talk about open quantum systems, i.e. subsystems with the ability to leak energy into its surroundings. Due to this exchange with other subsystems the formerly strict normalization constraint no longer has to be fulfilled for the subsystem (while it does remain for the global system). A distinction between pure and mixed states has to be introduced.

Luckily there are methods to treat open systems. The state of the system has to be described with a more general density operator instead of a state vector. The S.E. has to be modified with respect to this density operator and to account for dissipation from the subsystem under consideration. Additionally, the environment has to be modelled by reasonable approximations.

2.3.1 Density Operators

Unit state vectors, as used until now, are useful when describing single quantum states or pure ensembles of states. However, ensembles of states need not be pure. An ensemble may just as well be comprised by a mixture of different states of the system, $|\psi_i\rangle$, each with different weights, w_i. The pure ensemble is thus the special case where only one state is present, having the weight one. For a more general, and convenient, description of statistical ensembles the density operator (or density matrix), ρ, is used. It is defined as a linear combination of states, as

$$\rho \equiv \sum_i w_i \left|\psi_i\right\rangle \left\langle\psi_i\right| , \tag{12}$$

where the weights, w_i, fulfil the criteria $0 \leq w_i \leq 1$ and $\sum_i w_i = 1$. Eq. 12 implies that the density operator is a statistical mixture of pure states, where

the weights are classically statistical. Analogous to how state vectors evolve through unitary operations, see Eq. 86, unitary time evolution of density operators is described by

$$\rho' = \hat{U}\rho\hat{U}^{\dagger}. \tag{13}$$

2.3.2 Properties of the Density Operator

This overview of density operators is mainly based on sec.2.4 in [13] and sec.3.4 in [15]. Density matrices are positive operators with unity trace, due to

$$\mathrm{tr}(\rho) = \sum_i w_i \,\mathrm{tr}(|\psi_i\rangle \langle\psi_i|) = \sum_i w_i = 1 \tag{14}$$

and

$$\langle\zeta|\rho|\zeta\rangle = \sum_i w_i \langle\zeta|\psi_i\rangle \langle\psi_i|\zeta\rangle = \sum_i w_i |\langle\zeta|\psi_i\rangle|^2 \geq 0, \tag{15}$$

where ζ is an arbitrary vector in the Hilbert space.

While the trace of a density operator always equals one, it can readily be shown that the trace of the squared density operator does not. This measure is called purity, and takes its maximum value for pure ensembles and reduces the more mixed an ensemble is. The lower bound for the purity is the inverse of the dimensionality, d, of the system's Hilbert space. These boundaries can be summarized as

$$\frac{1}{d} \leq \mathrm{tr}(\rho^2) \leq \mathrm{tr}(\rho) = 1. \tag{16}$$

A pure ensemble always has the purity 1 as

$$\rho_p = |1\rangle\langle 1| = \begin{bmatrix} 1 & 0 \\ 0 & 0 \end{bmatrix} \Rightarrow \mathrm{tr}(\rho_p^2) = \mathrm{tr}(\rho_p) = 1, \tag{17}$$

while a maximally mixed ensemble, e.g $\rho_m = \frac{1}{2}|1\rangle\langle 1| + \frac{1}{2}|0\rangle\langle 0|$, yields the purity $\frac{1}{d}$ according to

$$\rho_m = \begin{bmatrix} 0.5 & 0 \\ 0 & 0.5 \end{bmatrix} \Rightarrow \mathrm{tr}(\rho_m^2) = \frac{1}{2} = \frac{1}{d}. \tag{18}$$

The Bloch sphere again appears instrumental, as it gives a geometrical interpretation of purity as well. Only pure state vectors will have its terminal point on the surface, while the whole volume makes up the space for mixed

states. A fully mixed state of a qubit, as described by ρ_m, is represented by the zero vector, $\vec{0}$, in the Bloch Sphere.

The diagonal elements of the density operator represent the populations of each eigenstate of the system. This can already be seen in Eqs. 17 and 18, and is validated by the examples:

$$\langle 1|\rho_p|1\rangle = \rho_{p11} = 1, \tag{19}$$

$$\langle 0|\rho_p|0\rangle = \rho_{p22} = 0 \tag{20}$$

and

$$\langle 1|\rho_m|1\rangle = \rho_{m11} = \frac{1}{2} = \rho_{m22} = \langle 0|\rho_m|0\rangle \,. \tag{21}$$

The expectation value of an operator $\hat{A}$, in a state $|\psi\rangle$, which is defined as $\langle \hat{A} \rangle_\psi \equiv \langle \psi|\hat{A}|\psi\rangle$, is only valid for pure, normalized state vectors. In the language of density operators the expectation value of an operator is instead defined as

$$\langle \psi \rangle_\rho \equiv \mathrm{tr}(\rho \hat{A}). \tag{22}$$

A more detailed mathematical review of the density operator is found in sec.19.3 of [9].

2.3.3 Liouville-von Neumann Equation

The density operator can also be used to describe time evolution of a system. As the density operator is a representation of a system which is time dependent, the operator itself is time dependent in accordance with

$$\rho(t) = \sum_i w_i \, |\psi_i(t)\rangle \, \langle \psi_i(t)| \,. \tag{23}$$

$|\psi_n(t)\rangle$ can be any arbitrary state, i.e. it does not have to be an eigenstate of the system. The states $|\psi_n(t)\rangle$ evolve according to the Schrödinger Equation, Eq. 95, as long as the system is closed. The time evolution of ensembles and the corresponding equation of motion is treated in [15] and [3]. In order to get the time derivative of $\rho(t)$ the chain rule is applied to Eq. 23, as:

$$\frac{\partial}{\partial t}\rho(t) = \sum_n p_n \left(-\frac{i}{\hbar}\right) \hat{H} \left|\psi_n(t)\right\rangle \left\langle\psi_n(t)\right| + \sum_n p_n \left(\frac{i}{\hbar}\right) \left|\psi_n(t)\right\rangle \left\langle\psi_n(t)\right| \hat{H} =$$
$$= -\frac{i}{\hbar}(\hat{H}\rho(t) - \rho(t)\hat{H}). \tag{24}$$

In the last part of the preceding equation the commutator between $\hat{H}$ and $\rho(t)$ appears, why it is practice to express the equation as

$$\frac{\partial}{\partial t}\rho(t) = -\frac{i}{\hbar}[\hat{H},\rho(t)]. \tag{25}$$

Equation 25 is called the Liouville-von Neumann equation and is the quantum analogue to the Liouville equation used in classical statistical mechanics.

The Liouville-von Neumann equation itself is not able to describe energy exchange with an environment, it is merely a statistical analogy to the state vector S.E. This description of the density operator is however an important step towards a more general description of a dissipative open quantum system.

2.3.4 Subsystems and the Reduced Density Operator

In order to treat composite quantum systems, i.e. systems with separate state spaces, the tensor product (or Kronecker product) is used. This section about tensor products and how to describe composite quantum systems is based on the sections 2.1.7, 2.2.8 and 2.4.3 in [13]. The tensor product, which is denoted by $\otimes$, creates a larger common vector space for the systems by extending the dimensionality of the space. The tensor product between two arbitrary state spaces $\mathcal{A}$ and $\mathcal{B}$ with dimensions m and n respectively create a vector space of dimension $m \cdot n$, i.e.

$$\mathbb{C}^m \otimes \mathbb{C}^n = \mathbb{C}^{m \cdot n}. \tag{26}$$

Now let the state spaces $\mathcal{A}$ and $\mathcal{B}$ represent two qubits, each qubit having a state space in $\mathbb{C}^2$. The resulting tensor product is a four dimensional state space. A state ket for a two qubit system thus has to be described by a four dimensional vector, as there are four different energy eigenstates of the system. For simplicity, the notation $|a\rangle \otimes |b\rangle = |ab\rangle$ is often used. The general action of the tensor product is explained as

$$A \otimes B \equiv \begin{bmatrix} A_{11}B & \dots & A_{1n}B \\ \vdots & \ddots & \vdots \\ A_{m1}B & \dots & A_{mn}B \end{bmatrix}, \tag{27}$$

where A is a matrix of dimensions $m \times n$ and B is a matrix of dimensions $p \times q$.

For example, two qubits in their ground states, $|0\rangle$, would give rise to the state vector

$$|00\rangle = \begin{bmatrix} 0 \\ 1 \end{bmatrix} \otimes \begin{bmatrix} 0 \\ 1 \end{bmatrix} = \begin{bmatrix} 0 \\ 0 \\ 0 \\ 1 \end{bmatrix} \tag{28}$$

acquired from the tensor product between the states. Consequently the density operator of a two qubit system is a 4×4 matrix. Keeping the same example as above, the resulting density matrix would be

$$\rho = |00\rangle\langle 00| = \begin{bmatrix} 0 & 0 & 0 & 0 \\ 0 & 0 & 0 & 0 \\ 0 & 0 & 0 & 0 \\ 0 & 0 & 0 & 1 \end{bmatrix}. \tag{29}$$

From this result it can again be noted that the diagonal elements can be interpreted as population of the energy eigenstates even when the density operator is describing a larger system. The probability of the system being in its ground state is of course unity, just as the matrix element ρ_{44} indicates.

Given a density operator describing a composite quantum system it is possible to restore information about single subsystems. This system is then represented by the so called reduced density operator which is obtained through a partial trace operation. Consider the same example state spaces as above, $\mathcal{A}$ and $\mathcal{B}$, containing vectors $|\psi_n\rangle$ and $|\phi_n\rangle$ respectively. The density operator describing this joint system can be denoted ρ_{AB}. The partial trace operation may then extract the density operator of only subspace $\mathcal{A}$, denoted ρ_A, as

$$\rho_A = \mathrm{tr}_B(\rho_{AB}). \tag{30}$$

The partial trace over system X, $\mathrm{tr}_X(\cdot)$, acts as it is only tracing over elements belonging to this system. The partial trace operation is defined as

$$\mathrm{tr}_B(|\psi_1\rangle\langle\psi_2| \otimes |\phi_1\rangle\langle\phi_2|) \equiv |\psi_1\rangle\langle\psi_2| \,\mathrm{tr}(|\phi_1\rangle\langle\phi_2|). \tag{31}$$

For a product state, $\rho_A \otimes \rho_B$, the relation in Eq. 30 becomes rather intuitive as the trace of each density matrix is unity:

$$\mathrm{tr}_B(\rho_{AB}) = \mathrm{tr}_B(\rho_A \otimes \rho_B) = \rho_A \,\mathrm{tr}(\rho_B) = \rho_A. \tag{32}$$

2.3.5 Environment Description

The system that is treated in this report will be divided into an open quantum subsystem associated some kind of macroscopic environment. A description of this environment makes it possible to proceed towards a general equation, describing the dynamics of this open quantum system. Complementary discussions regarding environments can be found in sec.8.2.2 of [13] and sec.3.1.3 of [3]. The environment will be modelled as a bosonic bath of e.g. the vibrational modes of phonons or an electromagnetic field. Initially the system, S and the environment E are taken to be in a product state,

$$\rho_{SE}(0) = \rho_S(0) \otimes \rho_E(0). \tag{33}$$

This is generally not true for all times. However, this assumption can be motivated since when a system is prepared in a specific state all correlations with the environment are eliminated. Hence, the total system can initially be described by a product state between the ancilla states of the principal system and an environment.

It is assumed that the total system $S + E$ is closed, while the system S is open for interactions with the environment. The dynamics of the reduced system will depend on internal dynamics as well as interactions with the environment. As stated in [2] and [3], the Hilbert space of the total system can be expressed as the tensor product between the Hilbert spaces of the included subsystems,

$$\mathcal{H}_{tot} = \mathcal{H}_S \otimes \mathcal{H}_E, \tag{34}$$

where $\mathcal{H}_S$ and $\mathcal{H}_E$ are the Hilbert spaces of the principal system and the environment respectively. The total Hamiltonian of a composite system can further be constructed as

$$\hat{H}_{tot}(t) = \hat{H}_S(t) \otimes \mathbb{1}_E + \mathbb{1}_S \otimes \hat{H}_E(t) + \hat{H}_I(t). \tag{35}$$

Here $\mathbb{1}_{S,E}$ are the identity matrices in each Hilbert space, $\mathcal{H}_S$ and $\mathcal{H}_E$. $\hat{H}_{S,E}$ are the Hamiltonians of the principal system and the environment

respectively. In this work the internal Hamiltonians, $\hat{H}_{S,E}$, will be time independent as no external drive is applied to the system. Except for the internal dynamics of each subsystem the interactions between the systems have to be represented as well, why $\hat{H}_I$ is the term representing these mutual effects. As a consequence of these system-environment interactions the reduced system dynamics can not be treated as unitary dynamics.

The environment will more specifically be referred to as a heat bath or a heat reservoir implying that it is large and considered a thermal equilibrium state. Large in this context means that it has an infinite number of degrees of freedom. This further means that the heat baths can be considered being in thermal equilibrium (or Gibbs states).

2.3.6 Master equation on Lindblad form

The Liouville-von Neumann equation is only valid for a closed system, for which it describes the unitary evolution of its internal dynamics. As mentioned above, the goal when working with a composite system is to in a valid way reduce the full description by discarding the environment from the calculations. Thus only bothering with the, generally non-unitary, evolution of the principal system. This can be viewed as tracing out the environment, and thus solely describing the internal dynamics of the subsystem together with a system-environment interaction. The density operator for the principal subsystem is obtained by the relations

$$\rho_{SE}(t) = \hat{U}(t)\rho_{SE}(0)\hat{U}^\dagger(t) \tag{36}$$

and

$$\rho_S(t) = \mathrm{tr}_E\left(\rho_{SE}(t)\right). \tag{37}$$

Eqs. 37 and 33 lead back to the so called Stinespring dilation, discussed in [17], which assures that every completely positive and trace preserving map, $\Phi\colon \rho_S \to \rho'_S$, can be constructed through only a tensor product between the principal state, ρ_S and the environment state, ρ_E, a global unitary operator, $\hat{U}$ and the partial trace over the environment, tr_E as

$$\rho'_S = \Phi(\rho_S) = \mathrm{tr}_E\left(\hat{U}\rho_S \otimes \rho_E\hat{U}^\dagger\right). \tag{38}$$

To treat this reduced density operator a so called quantum master equation is utilized. A quantum master equation is an equation which describes the continuous-time evolution of a quantum system through its density matrix. The equation describes the transitions among a probabilistic set of states

through some transition rate. The master equation may also include system-environment interactions, giving access to the non-unitary time evolution of an open quantum system. Unlike a classical master equation, the quantum master equation also considers the off-diagonal elements of the density matrix, which represent quantum coherence.

When discussing master equations it is practical to define a superoperator, $\mathcal{S}$. The term superoperator emphasizes that it is an operator acting on another operator in order to produce a new operator. As an example, the superoperator corresponding to the case of the Liouville-von Neumann equation is defined, through acting on the density operator, as

$$\mathcal{S}\rho(t) = -\frac{i}{\hbar}[\hat{H},\rho(t)]. \tag{39}$$

In order to fit the reduced density operator of Eq. 37 into an adequate equation of motion it is first noted that the internal dynamics of the principal system still are unitary, and obey the Liouville-von Neumann equation. In addition, some system specific dissipation terms, $\mathcal{D}(\rho)_i$, have to be appended to account for the dynamics arising from the system-environment interactions. These terms give rise to the non-unitary evolution of the principal system. The superoperator, $\mathcal{S}$, can now instead be written as

$$\mathcal{S}\rho_S(t) = -\frac{i}{\hbar}[\hat{H}_S,\rho_S(t)] + \sum_i \mathcal{D}_i(\rho_S(t)), \tag{40}$$

where it should be noted that the dissipators, $\mathcal{D}_i$, act as superoperators themselves. More theory regarding quantum master equations is found in sec.8.4.1. of [13] and ch.3 in [3].

It is explained in e.g. [3], [13], [6] and [14] that some assumptions have to be made about the system in order to arrive at a solvable master equation. The Born approximation and the Markov approximation are often grouped and called the Born-Markov approximation. In addition it is necessary to make the so called rotating wave approximation in order to guarantee that the resulting master equation describes a generator for a quantum dynamical semi-group.

- *The Born approximation* assumes a weak coupling between the principal system and the heat bath. This ensures that the impact of the interaction, $\hat{H}_{SE}$, on the heat bath density matrix, ρ_E, is negligible. NB, excitations from the thermal state of the heat bath are allowed as long as they can be considered small. This further leads to the approximation that the total system at time t can be constructed by the tensor product $\rho_{SE}(t) = \rho_S(t) \otimes \rho_E$.

- *The Markov approximation* imply that the decay time for excitations in the heat bath, τ_E must be shorter compared to the relaxation time of the reduced system, τ_S. As the name suggests the Markov approximation stems from the Markov property of probability theory - a stochastic process which is memoryless. $\tau_E \ll \tau_S$ ensures that deviations in the environment state are too short to be resolved. This approximation is valid for a very large environment which contains a continuum of modes.

- *The rotating wave approximation* is performed by averaging over and neglecting rapid oscillations in the master equation. The condition for the rotating wave approximation to be valid is that the relaxation time of the system is large compared to the inverse of the frequency differences involved.

It was first demonstrated in [12] that the most general form of a Markovian quantum master equation is that on the Lindblad form, also called the Lindblad equation,

$$\frac{d}{dt}\rho_S(t) = \mathcal{L}\rho_S(t), \tag{41}$$

with its corresponding Lindblad superoperator, $\mathcal{L}$,

$$\mathcal{L}\rho_S = -\frac{i}{\hbar}[\hat{H}_S,\rho_S] + \sum_k \left(\hat{L}_k \rho_S \hat{L}_k^\dagger - \frac{1}{2}\{\hat{L}_k^\dagger \hat{L}_k,\rho_S\} \right). \tag{42}$$

In the equation above $\{\cdot,\cdot\}$ denotes the anti-commutator: $\{x,y\} = xy + yx$. The operators, $\hat{L}_k$, are termed Lindblad operators.

The Lindblad operators are system specific operators containing a description of some process paths, $\hat{A}_{i,j}$, arising from the interaction between the principal system and the environment. With this picture in mind, the Lindblad operators can instead be labelled accordingly as $\hat{L}_{i,j}$. Additionally, each process is associated with a corresponding rate, $\Gamma_{i,j}$. There is a wide range of Lindblad operators, but those relevant for this thesis are related to transitions between energy eigenstates of the system. They take the general form

$$\hat{L}_{i,j} = \sqrt{\Gamma_{i,j}}\hat{A}_{i,j}. \tag{43}$$

The operators $\hat{A}_{i,j}$ are ladder operators describing energy transitions within the qubits: $\hat{A}_{i,j} = |i\rangle\langle j|$. Further reading about the Lindblad form and the Lindblad operators is readily found in e.g. sec.4.1 in [17], sec.8.4 in [4] and [2].

2.4 Quantum Thermodynamics

Thermodynamics has been a major branch of physics for several centuries. The fundamental objectives of thermodynamics are how heat and temperature is related to energy and work. The urge to make engines and other thermodynamic machines more effective has made the field utterly important to modern history. Classical thermodynamics rely on statistical and empirical results, with the four laws of thermodynamics acting as a rigid framework.

"With ultrafast experimental control of quantum systems and engineering of small environments pushing the limits of conventional thermodynamics, the central goal of quantum thermodynamics is the extension of standard thermodynamics to include quantum effects and small ensemble sizes."
Vinjanampathy, S., Anders, J. p.2 [17]

With the recent possibilities to engineer and control mesoscopical and microscopical physical systems a need to revisit the well accepted framework of thermodynamics emerged. This is due to the facts that the small ensemble sizes challenge the statistical approach and that quantum phenomena appear beyond the limits of classical physics. It is stated in [17] that the main goal of quantum thermodynamics is to stretch conventional thermodynamics to encompass microscopical systems as well. Besides this, they express a wish to better understand thermodynamic properties of quantum systems in order to develop applications into even smaller scales. One example is the desire to investigate the performance of quantum thermal machines, as in this thesis where a quantum heat pump will be evaluated.

2.4.1 Bose–Einstein statistics and Detailed Balance

The rates introduced in Eq. 43, $\Gamma_{i,j}$, are determined by a coupling strength, γ, and a distribution function, n. The rates can be expressed as

$$\Gamma_{i,j} = \gamma \cdot n(\Delta E_{i,j}), \tag{44}$$

where $\Delta E_{i,j}$ is the energy difference between the states $|i\rangle$ and $|j\rangle$. For the system of this thesis, with bosonic heat reservoirs, the transitions obey the Bose–Einstein statistics. The expected occupancy level, n, of an energy eigenstate, E_i, is given as

$$n(E_i) = \frac{1}{e^{E_i\beta} - 1}. \tag{45}$$

β equals $(k_B T)^{-1}$, where k_B is Boltzmann's constant and T is the absolute temperature.

Since the system-environment interactions go both ways there is also a need to define a direction for the processes by assigning a sign to the Lindblad operators:

$$\begin{aligned} \hat{L}^{-}_{i,j} &= \sqrt{\Gamma^{-}_{i,j}}\hat{A}_{i,j} \\ \hat{L}^{+}_{i,j} &= \sqrt{\Gamma^{+}_{i,j}}\hat{A}^{\dagger}_{i,j}. \end{aligned} \tag{46}$$

The rates, $\Gamma^{\pm}_{i,j}$ are related to each other through the principle of detailed balance. According to [15], detailed balance is a symmetry relation between absorption and emission. In more general terms, the principle states that in any kinetic system every elementary process has to be counteracted by its reverse process in order to maintain thermodynamic equilibrium. This symmetry effectively reads as

$$\frac{\Gamma^{-}_{i,j}}{\Gamma^{+}_{i,j}} = e^{\Delta E_{i,j}\beta}. \tag{47}$$

With the use of Eq. 44 and Eq. 47, the expressions in Eq. 46 can be recast into

$$\hat{L}^{-}_{i,j} = \sqrt{\gamma \cdot (n(\Delta E_{i,j}) + 1)}\hat{A}_{i,j} \tag{48a}$$

and

$$\hat{L}^{+}_{i,j} = \sqrt{\gamma \cdot n(\Delta E_{i,j})}\hat{A}^{\dagger}_{i,j}. \tag{48b}$$

A more thorough explanation of detailed balance, and how the Bose–Einstein function (as well as the Fermi–Dirac function) can be derived from that principle, can be found in [11].

2.4.2 Work and heat

Energy, and how it changes over time, is clearly of vital interest when studying thermodynamics. In accordance with Eq. 22, the average internal energy of a system, U, is identified as

$$U = \langle E \rangle_{\rho} = \mathrm{tr}(\rho \hat{H}). \tag{49}$$

How the average energy changes over time, ΔU, is a consequence of the time evolution of the system's state, $\rho(t)$, and the Hamiltonian, $\hat{H}(t)$. For $t \in [t_1,t_2]$ the energy change can be written as

$$\Delta U = \mathrm{tr}\left(\rho(t_2)\hat{H}(t_2)\right) - \mathrm{tr}\left(\rho(t_1)\hat{H}(t_1)\right). \tag{50}$$

According to the first law of thermodynamics,

$$\Delta U = Q + W, \tag{51}$$

changes in a system's internal energy are always comprised of heat, Q, and work, W. Thus, proper quantum representations of these quantities have to be found. It is fruitful to differentiate Eq. 49, as showed in [10], like

$$\frac{d}{dt}U = \frac{d}{dt}\left(tr(\rho\hat{H})\right) = \mathrm{tr}\left(\frac{d\rho}{dt}\hat{H}\right) + \mathrm{tr}\left(\rho\frac{d\hat{H}}{dt}\right), \tag{52}$$

in order to get two distinguishable parts.

Work can be performed on the system only by altering the Hamiltonian acting on the system, $\frac{d\hat{H}}{dt}$. Hence, the second term above is identified as the temporal change in energy stemming from work. The change of the state of the system, $\frac{d\rho}{dt}$, due to e.g. interactions with an environment or thermalisation, is associated with the contribution from heat. In the quantum regime, the definitions for work is

$$\langle W\rangle = \int_{t_1}^{t_2} \mathrm{tr}\left(\rho\frac{d\hat{H}}{dt}\right)dt \tag{53}$$

and the definition of heat is consequently

$$\langle Q\rangle = \int_{t_1}^{t_2} \mathrm{tr}\left(\frac{d\rho}{dt}\hat{H}\right)dt. \tag{54}$$

Work and heat in this context are ensemble averages, $\langle\cdot\rangle$, due to the trace operation performed in Eq. 49. With the definitions above work is added to a system if $\langle W\rangle > 0$ and heat is flowing into a system if $\langle Q\rangle > 0$.

The previous Eqs. 50, 51, 53 and 54 can be merged into a common expression, as also demonstrated in [17], in order to clarify the connection among them in accordance with

$$\begin{aligned}\langle Q\rangle + \langle W\rangle = \int_{t_1}^{t_2} \mathrm{tr}\left(\frac{d\rho}{dt}\hat{H}\right)dt + \int_{t_1}^{t_2} \mathrm{tr}\left(\rho\frac{d\hat{H}}{dt}\right)dt = \\ = \int_{t_1}^{t_2} \frac{d}{dt}\,\mathrm{tr}(\rho\hat{H})dt = \mathrm{tr}\left(\rho(t_2)\hat{H}(t_2)\right) - \mathrm{tr}\left(\rho(t_1)\hat{H}(t_1)\right) = \Delta U.\end{aligned} \tag{55}$$

2.4.3 Quantum Thermal Machines

The concept of quantum thermal machines was first demonstrated in 1959 when H.E.D. Scovil and E.O. Schulz-DuBois showed how the three-level maser can be thought of as a quantum heat engine (and reversibly as a refrigerator). In the same article [16] they also showed that the efficiency of this setup was limited by the Carnot efficiency, the upper bound for any classical thermal machine.

"The principal conceptual difference between these and conventional heat engines is that in the 3-level maser one is concerned with the discrete energy levels of a particle's internal energy whereas in a conventional heat engine one is concerned with the continuous spectrum of energies associated with external motion of the working substance."
Scovil H.E.D. and Schulz-DuBois E.O. p.1 [16]

A significant part of applied thermodynamics regards the field of thermal machines. The quest has long been to optimize heat engines, and heat pumps. A heat engine is a system which utilizes thermal baths of different temperatures in order to extract work. It takes heat from the hot reservoir, extracts work in the process and delivers a smaller amount of heat to the cold reservoir, see Fig. 2a. The reverse process, a heat pump or refrigerator, requires some input to transfer heat in the reverse direction, see Fig. 2b.

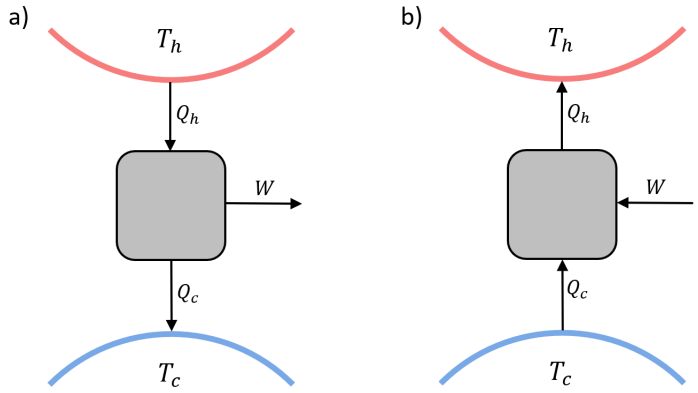

Figure 2: a) schematically illustrates a thermal heat engine. Heat, Q_h flows from the hot reservoir, T_h, into the engine. The engine is capable of extracting work, W, and residual energy is deposited to the cold reservoir, T_c, in the form of heat, Q_c. $\Delta U = Q_h - Q_c - W = 0$, why $W = Q_h - Q_c$. b) shows instead the basic operation of a refrigerator. The same concepts apply, but the directions of heat and work flow are reversed.

In this thesis, the main objective is to simulate a continuous absorption-driven quantum heat pump.

- The device is *continuous* in the sense that the process is not divided into different distinct steps, cf. Carnot or Otto cycles. The heat transfer through the device is only governed by the energy transitions embedded in the rate equations, Eq. 44, and consequently the Lindblad operators, Eq. 48.
- The term *absorption-driven* is due to the fact that no external work source will be used. Instead of a work supply, as Fig. 2b suggests, the heat pump is driven by an additional supply of heat. This heat source will be modelled as a third heat reservoir, and since it acts as drive for the system it will be labelled work reservoir, T_w.
- This thermal machine becomes *quantum* since the system consists of two qubits, which certainly have discrete energy levels. This eventually means that the dynamics of the system has to be evaluated through a quantum master equation, namely the Lindblad equation 41.

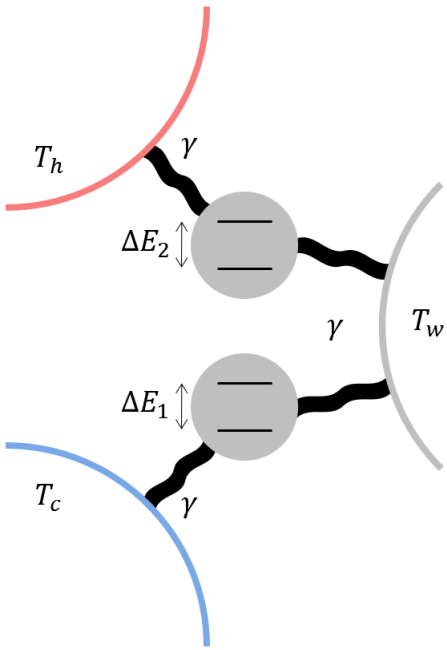

Figure 3: A two-qubit absorption driven heat pump. Both qubits are coupled to the work reservoir while each qubit couples to either the hot or the cold reservoir. The coupling factors, γ, are assumed to be constant for all connections.

The configuration of this heat pump is visually explained in Fig. 3. In order to ensure the Markov property it is assumed that $\gamma \ll T_c, \Delta E_1$. The energies involved can also be described by assigning the ground states of each qubit a common energy, i.e. zero. In this case the energies of the excited states will be denoted E_c and E_h respectively. Additionally the energy provided by the work reservoir is $E_h - E_c = E_w$. An overview of quantum thermal machines can be found in sec.6 of [17].

2.4.4 Figures of Merit

In order to evaluate and benchmark these thermal machines it is essential to define some figures of merit. According to [8], the coefficient of performance (COP), η, and the cooling power are two important parameters in the case of refrigerators. The COP for a general heat pump in chiller mode is defined as

$$\eta = \frac{\dot{Q}_c}{\dot{W}}, \tag{56}$$

while the cooling power is defined as the heat flow out from the cold reservoir, $\dot{Q}_c$, neglecting the efficiency of the overall process. In the case of absorption refrigerators the work input is substituted for a heat current mediated by the work reservoir, $\dot{Q}_w$. In this case η is instead defined as

$$\eta = \frac{\dot{Q}_c}{\dot{Q}_w} = \frac{\dot{Q}_c}{\dot{Q}_h - \dot{Q}_c}. \tag{57}$$

The COP can be thought of as a measure of efficiency. However, since $\eta > 1$ for a heat pump in heater mode, the term efficiency is not preferred.

A quantum heat pump is governed by the four thermodynamic laws once it reaches steady-state, as stated in [6]. This statement further leads to the conclusion that their performance, like their classical analogues, are restricted by the Carnot limit, η_C. To reach this conclusion the first law of thermodynamics, Eq. 51, is recast into the sum of all heat currents present in the system, namely

$$\Delta U = \dot{Q}_c + \dot{Q}_h + \dot{Q}_w = 0. \tag{58}$$

The second law of thermodynamics can be formulated in the form of a Clausius inequality as

$$\frac{\dot{Q}_c}{T_c} + \frac{\dot{Q}_h}{T_h} + \frac{\dot{Q}_w}{T_w} \leq 0, \tag{59}$$

which is equivalent to saying that the entropy production in the heat baths cannot be negative. See [6] for more details on this matter. The three terms in Eq. 59 only describe the entropy changes in the reservoirs and does not take the active medium into consideration. This is perfectly fine when the law describes the system in steady state operation, when the the energy of the qubits is invariant. To study the transient behaviour of the system by means of the second law the entropy change of the reduced system also has to be included. The quantum analogue of the Gibbs entropy from thermodynamics (and the Shannon entropy from information theory) is the so called von Neumann entropy. This quantity is defined as

$$S = -\operatorname{tr}(\rho \ln \rho), \tag{60}$$

which makes the second law take the form

$$\sum_i \Delta S_i = \frac{dS_S}{dt} - \frac{\dot{Q}_c}{T_c} - \frac{\dot{Q}_h}{T_h} - \frac{\dot{Q}_w}{T_w} \geq 0, \tag{61}$$

where S_S is the entropy of the reduced system.

By combining Eqs. 58 and 59 one can reach an expression for $\frac{\dot{Q}_c}{\dot{Q}_w}$, which defines an upper bound for the COP. This limit takes the form of

$$\eta = \frac{\dot{Q}_c}{\dot{Q}_w} \leq \frac{T_c(T_w - T_h)}{T_w(T_h - T_c)}. \tag{62}$$

Thus the Carnot limit for a refrigerator operating between three heat reservoirs, η_C, can further be defined as

$$\eta_C = \frac{(T_w - T_h)T_c}{(T_h - T_c)T_w} = \frac{\beta_h - \beta_w}{\beta_c - \beta_h}. \tag{63}$$

Since the Carnot limit sets a fundamental limit of performance it is often more explicit to express the COP as a fraction of the Carnot COP,

$$\frac{\eta}{\eta_C} \leq 1, \tag{64}$$

where it is easier to see how close to the theoretical limit the performance reaches.

2.4.5 Conditions for Cooling

In [6] some criteria are presented that have to be met in order for the heat pump configuration in Fig. 3 to achieve a cooling effect. The relations $E_h > E_c$ and $T_w > T_h > T_c$ apply in order for the machine to operate as

a refrigerator. These conclusions are deduced from the probability for each transition to occur, i.e. the rate equations 44. These rates, $\Gamma_{c,w,h}$, imply that the distribution functions, $n_{c,w,h}$ of Eq. 45, have to be ordered in the same way (since the coupling, γ, is constant and assumed to be the same for all connections).

In fact a stronger condition for the relation between the energy splittings in each qubit, $E_{c,h}$, can be formulated. It can be deduced that the ratios between all heat currents are proportional to the corresponding ratio between the energy transitions involved, see Fig. 4. This is motivated by breaking down the heat currents into the discrete transitions giving rise to the cooling process. Each excitation over E_c results in one excitation over E_h with the assist of the input E_w, or vice versa. No other transitions are allowed within the system, leading to

$$\left|\frac{\dot{Q}_i}{\dot{Q}_j}\right| = \frac{E_i}{E_j}, \tag{65}$$

for $i,j \in \{c,h,w\}$.

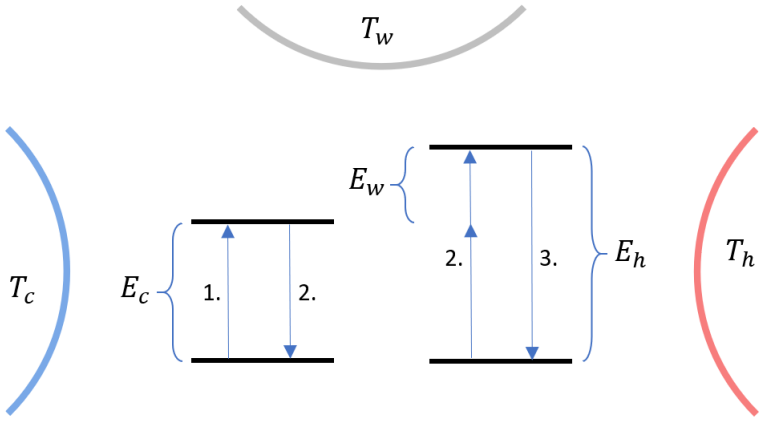

Figure 4: The figure schematically illustrates the cooling process in terms of discrete energy transitions. 1. The cold reservoir provides energy in order to excite the first qubit. This creates the heat current, $\dot{Q}_c > 0$. When this excited state relaxes to its ground state this energy is provided to the other qubit. The additional energy required, due to the difference E_w, is provided by the work reservoir and gives rise to $\dot{Q}_w > 0$. 3. The energy released when the second qubit relaxes down to its ground state is deposited into the hot reservoir. This energy leaves the active medium and therefore gives rise to $\dot{Q}_h < 0$.

By combining Eqs. 59 and 65 a relation between E_c and E_h can be formulated,

$$E_c \leq E_c^{max} \equiv \frac{T_c(T_w - T_h)}{T_h(T_w - T_c)} E_h, \tag{66}$$

defining a cooling window for the system. This equation also strengthens the statement that $T_w > T_h > T_c$, since we need a positive E_c^{max}.

The thermodynamic theory provided so far assumes that the system has reached a steady-state operation. However, the qubits, which have been referred to as the reduced or principal system, are initially prepared in an (arbitrary) ancilla state. The state of the qubits will gradually thermalise and reach this steady-state with the heat reservoirs, in which the machine can be described by the thermodynamic laws.

3 Methods

The method for this project has been to numerically simulate a quantum heat pump, as described in Fig. 3, in MATLAB. The code has been written specifically for this project by defining an initial state of the system and studying the dynamics over time. A Hamiltonian for the principal system was defined, as well as the Lindblad operators governing the environment interactions. From this, a quantum master equation on Lindblad form could be defined, with which the time evolution of the reduced system density matrix could be studied. The heat currents were identified along the time evolution, and at some point, approaching steady-state, they were considered stationary. These stationary heat currents were utilized to evaluate the performance of the heat pump in terms of COP and cooling power. These steps will be explained in more detail in the following sections. All calculations, data handling and graphic output has been performed in MATLAB.

The initial aim of this project was to describe a heat pump consisting of two coherent qubits operating between only two heat reservoirs, driven with an external work input. However, no protocol was found for that set up to work properly, why the project aim was altered. The inspiration for a quantum thermal machine is mainly taken from the 3-level maser action studied by H. E. D. Scovil and E. O. Schulz-DuBois in "Three-level Masers as Heat Engines", [16]. The more specific idea of an absorption driven refrigerator is based on the article "Quantum-enhanced absorption refrigerators" by L.A. Correa et al., [6].

3.1 Initial State of the System

The system in question consists of two qubits, each with a Hilbert space $\mathbb{C}^2$, weakly coupled to three heat reservoirs with different temperatures, each in a Gibbs state. To study the open system dynamics of the qubits the degrees of freedom of the heat baths are traced out, resulting in a reduced density matrix, ρ_s, with a Hilbert space $\mathbb{C}^4$. Full experimental control over the ancilla state is assumed, which also leads to an initial separability property between the principal system and the environment. This makes it possible to directly define the state of the qubits as

$$|\psi_1\psi_2\rangle = \begin{bmatrix} a \\ b \end{bmatrix} \otimes \begin{bmatrix} c \\ d \end{bmatrix}, \tag{67}$$

and the corresponding density matrix

$$\rho_S = |\psi_1\psi_2\rangle \langle\psi_1\psi_2| . \tag{68}$$

The normalization condition, $a^2 + b^2 = c^2 + d^2 = 1$, applies, which further leads to the density matrix having unity trace, $\mathrm{tr}(\rho_S) = 1$

3.2 Hamiltonian

The internal dynamics of the principal system are governed by a Hamiltonian, $\hat{H}_S$. Since the work reservoir was added to the system, no coherent coupling between the qubits is present. All interaction between the qubits is mediated by the work reservoir through incoherent dissipation, why the only thing the Hamiltonian need to define is the energy levels present in the principal system. This can be expressed by defining the energy differences in each qubit, E_1 and E_2 and using the generators, shown in table 1. Since no work is performed on the system the Hamiltonian is time-independent and takes the form

$$\hat{H}_S = \frac{E_1}{2} \cdot D_{30} + \frac{E_2}{2} \cdot D_{03}. \tag{69}$$

This is analogous to using the σ_z matrix for the Hamiltonian of a single qubit. This is done since the σ_z matrix has the eigenvectors

$$\psi_{z+} = |1\rangle = \begin{bmatrix} 1 \\ 0 \end{bmatrix} \quad \text{and} \quad \psi_{z-} = |0\rangle = \begin{bmatrix} 0 \\ 1 \end{bmatrix} \tag{70}$$

By simply taking the tensor product of the σ_z matrix and identity matrix, $\mathbb{1}_2$, Eq. 70 is extended to the 4 dimensional Hilbert space of two qubits. The matrices D_{30} and D_{03} are acquired through the relations:

$$\sigma_z \otimes \mathbb{1}_2 = \begin{bmatrix} 1 & 0 \\ 0 & -1 \end{bmatrix} \otimes \begin{bmatrix} 1 & 0 \\ 0 & 1 \end{bmatrix} = \begin{bmatrix} 1 & 0 & 0 & 0 \\ 0 & 1 & 0 & 0 \\ 0 & 0 & -1 & 0 \\ 0 & 0 & 0 & -1 \end{bmatrix} = D_{30} \tag{71a}$$

and

$$\mathbb{1}_2 \otimes \sigma_z = \begin{bmatrix} 1 & 0 \\ 0 & 1 \end{bmatrix} \otimes \begin{bmatrix} 1 & 0 \\ 0 & -1 \end{bmatrix} = \begin{bmatrix} 1 & 0 & 0 & 0 \\ 0 & -1 & 0 & 0 \\ 0 & 0 & 1 & 0 \\ 0 & 0 & 0 & -1 \end{bmatrix} = D_{03}. \tag{71b}$$

3.3 Dissipators

The dissipators acting on the reduced system, together with the Liouville-von Neumann term, take the Lindblad form shown in Eq. 42. More specifically each dissipator, $\mathcal{D}_i$, can be described as

$$\mathcal{D}_c\rho_S = \Gamma_c^+ \left(\sigma_c^+\rho_S\sigma_c^- - \tfrac{1}{2}\{\sigma_c^-\sigma_c^+,\rho_S\}\right) + \Gamma_c^- \left(\sigma_c^-\rho_S\sigma_c^+ - \tfrac{1}{2}\{\sigma_c^+\sigma_c^-,\rho_S\}\right), \tag{72a}$$

$$\mathcal{D}_h\rho_S = \Gamma_h^+ \left(\sigma_h^+\rho_S\sigma_h^- - \tfrac{1}{2}\{\sigma_h^-\sigma_h^+,\rho_S\}\right) + \Gamma_h^- \left(\sigma_h^-\rho_S\sigma_h^+ - \tfrac{1}{2}\{\sigma_h^+\sigma_h^-,\rho_S\}\right) \tag{72b}$$

and

$$\mathcal{D}_w\rho_S = \Gamma_w^+ \left(\hat{A}_w\rho_S\hat{A}_w^\dagger - \tfrac{1}{2}\{\hat{A}_w^\dagger\hat{A}_w,\rho_S\}\right) + \Gamma_w^- \left(\hat{A}_w^\dagger\rho_S\hat{A}_w - \tfrac{1}{2}\{\hat{A}_w\hat{A}_w^\dagger,\rho_S\}\right), \tag{72c}$$

where the indices c,h,w indicate if the dissipation refers to the cold, hot or work reservoir. For the dissipation regarding the hot and cold reservoirs the operators $\hat{A}_{i,j}$ and $\hat{A}_{i,j}^\dagger$, from Eq. 46, are defined as the lowering ($\sigma_{c,h}^-$) and raising ($\sigma_{c,h}^+$) operators respectively. The dissipation mediated by the work reservoir acts a bit differently. The operators governing that process are defined as

$$\hat{A}_w = \sigma_h^+\sigma_c^- \tag{73a}$$

and

$$\hat{A}_w^\dagger = \sigma_c^+\sigma_h^-, \tag{73b}$$

since one qubit is always being excited when the other is being de-excited.

3.4 Solving the Lindblad Equation

When the internal Hamiltonian, $\hat{H}_S$, as well as the dissipators, $\mathcal{D}_i$, are defined, the complete Lindblad equation is specified as

$$\frac{d}{dt}\rho_S(t) = -\frac{i}{\hbar}[\hat{H}_S,\rho_S(t)] + \sum_i \mathcal{D}_i\rho_S(t). \tag{74}$$

Even though the master equation is continuous in time, the numerical solution approximates time evolution of the density matrix with discrete time steps. The density matrix, $\rho_S(t)$, is vectorized as

$$\rho_S = \begin{bmatrix} \rho_{11} & \cdots & \rho_{14} \\ \vdots & \ddots & \vdots \\ \rho_{41} & \cdots & \rho_{44} \end{bmatrix} \rightarrow \tilde{\rho}_S = \begin{bmatrix} \rho_{11} \\ \rho_{12} \\ \vdots \\ \rho_{43} \\ \rho_{44} \end{bmatrix} \tag{75}$$

in order to rewrite the Lindblad equation according to

$$\frac{d\rho_S}{dt} = \mathcal{L}\rho_S \rightarrow \frac{d\tilde{\rho}_S}{dt} = \mathcal{M}\tilde{\rho}_S. \tag{76}$$

The matrix $\mathcal{M}$ is now a 16×16 single left acting operator acting on the vectorized density operator, $\tilde{\rho}_S$. The formal solution of the new expression is, in line with Eq. 96,

$$\tilde{\rho}_S(t+dt) = e^{\mathcal{M}dt} \cdot \tilde{\rho}_S(t). \tag{77}$$

To simplify the calculations, and get rid of the matrix exponential, Eq. 77 can be expanded around t and be represented as

$$\tilde{\rho}_S(t+dt) \approx \tilde{\rho}_S(t) + \mathcal{M}\tilde{\rho}_S(t)dt. \tag{78}$$

This Taylor expansion, up to the first order of dt, introduces restrictions in the resolution of the time evolution. All contributions of higher orders of dt are neglected in each time step, which means that this error is potentially stacked over time. By comparing the results of different sized time steps it is however possible to choose an adequate, sufficiently small, dt.

The validity of the calculations can be checked in several ways. For example, the simulation is not allowed to progress if the density matrix has any negative eigenvalues, thus checking its positivity.

3.5 Heat currents

In steady state operation the internal energy change in the principal system equals zero, in line with Eq. 58. By noting that the Hamiltonian of the system is constant in time we know that no work contributes to ΔU, since $\frac{d\hat{H}_S}{dt} = 0$. By also noting that $\frac{d\rho_S}{dt} = \mathcal{L}(\rho_S)$, the resulting change in internal energy can be expressed as

$$\Delta U = \int_{t_1}^{t_2} \mathrm{tr}\left(\mathcal{L}\rho_S(t)\hat{H}_S\right) dt. \tag{79}$$

This expression can be divided into heat contributions from the different heat reservoirs. The heat contributions per time unit, $\dot{Q}_i$, linked to a specific heat bath, $i \in \{c,h,w\}$, are

$$\dot{Q}_i = \mathrm{tr}\left(\hat{H}_S\left(-\frac{i}{\hbar}[\hat{H}_S,\rho_S] + \mathcal{D}_i\rho_S(t)\right)\right). \tag{80}$$

The laws of thermodynamics, as well as their quantum analogues, apply in steady state systems. During the process of thermalisation $\Delta U \neq 0$, why the first law can be used to determine when the system approaches steady state. This concept is used to terminate the simulation at a point in time where the sum of heat currents is tolerably small and the currents can be considered invariant. The limit is chosen to be

$$\sum_i |\dot{Q}_i| \leq 0.01 \cdot E_c \cdot \gamma, \tag{81}$$

thus depending on the energy scale of the specific system. In this way the figures of merit for each simulation become comparable.

Each heat flux, $\dot{Q}_i$, is a sum of two contributing fluxes, q_1 and q_2, as

$$|\dot{Q}_i| = E_i(q_1 + q_2), \tag{82}$$

where the indicies $i \in \{c,h,w\}$ imply which reservoir the heat is associated with. $q_{1,2} > 0$, $\dot{Q}_{c,w} > 0$ and $\dot{Q}_h < 0$. This was shown in [6], where an expression for $q_1 + q_2$ in steady state also was derived. It was found by studying the subspaces of the transitions that each heat bath drive, and finally appears as

$$q_1 + q_2 = \langle 1_h 0_c|\mathcal{L}_w\rho_S(\infty)|1_h 0_c\rangle\,, \tag{83}$$

where

$$\mathcal{L}_w\rho_S = -\frac{i}{\hbar}[\hat{H}_S,\rho_S] + \mathcal{D}_w\rho_S. \tag{84}$$

The Eqs. 82 and 83 were used in order to calculate the stationary heat currents in the system, approximating $\rho_S(\infty)$ with the density matrix acquired at the breaking point of each simulation.

4 Results and Analysis

The results from simulations, including various validity checks for the program, are presented and analysed in this section.

4.1 Populations and coherences

The system generally do not start in equilibrium with the environment. An excited ancilla state of the system, e.g. $|1_c 1_h\rangle$, will gradually relax towards a stable state. Qubits prepare in the ground state, $|0_c 0_h\rangle$, will conversely be excited due to the energy provided from the surrounding heat reservoirs. These examples are illustrated in Figs. 5a and 5b respectively.

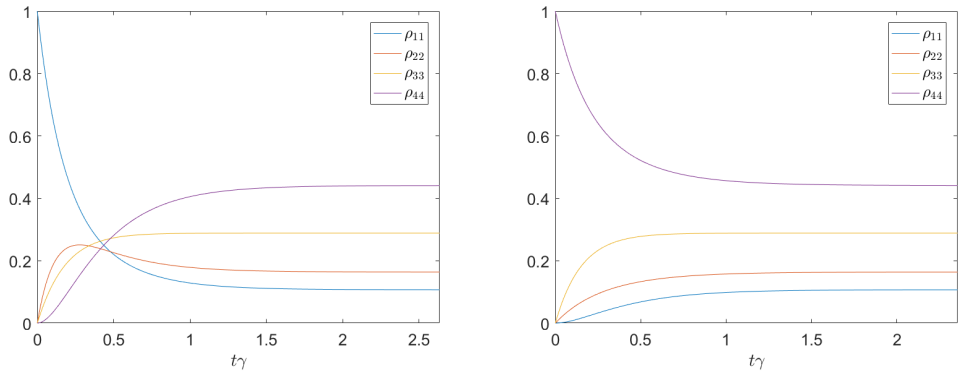

(a) Initial state $|1_c 1_h\rangle$ *(b) Initial state* $|0_c 0_h\rangle$

Figure 5: The figures show the time evolution of the state of the principal system from two different ancilla states. The remaining parameters used for both simulations were: $\gamma = 0.01$, $\beta_c = \frac{1}{2}$, $\beta_h = \frac{1}{12}$, $\beta_w = \frac{1}{20}$, $E_c = 0.95 \cdot E_c^{max}$ *and* $E_h = \frac{1}{\beta_h}$. *E_w is always obtained according to the resonance condition,* $E_w = E_h - E_c$.

The transient behaviours displayed in the figures above agree with expectations. For example, the population ρ_{44} correspond to the joint ground state $|0_c 0_h\rangle$, which naturally should be the most probable. It should also be noted that the final state of these examples are identical, even though the initial states differ. This is also expected since all other system parameters are chosen the same and thus generate the same steady state behaviour.

If the initial state is chosen to be a mixed state, some off-diagonal elements of the density matrix will be non-zero. Since no coherent coupling is present in the system these coherences will decay over time, which is demonstrated in Fig. 6. By for example starting in a Bell state,

$$|\beta_{00}\rangle = \frac{|00\rangle + |11\rangle}{\sqrt{2}}, \tag{85}$$

some non-zero elements are found. As expected, this choice of ancilla state does not influence the resulting populations. It is the use of a quantum master equation (i.e. the Lindblad equation) that enables tracking of all elements of the density matrix.

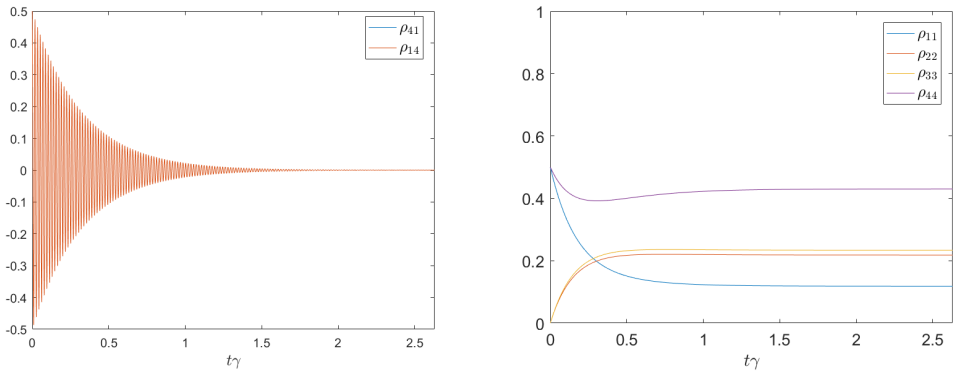

(a) Initial state $|\beta_{00}\rangle$ *(b) Initial state $|\beta_{00}\rangle$*

Figure 6: By choosing the system to start in a mixed state, in this case $|\beta_{00}\rangle$, some off-diagonal elements will be non-zero. Figure 6a shows these coherences are damped over time, with ρ_{14} and ρ_{41} overlapped. Figure 6b is included to verify that the populations approach steady-state with this choice of initial state as well.

4.2 Trace Preservation and Purity

The mapping performed through the Lindblad equation has to be completely positive and trace preserving. The positivity condition is readily checked by demanding exclusively positive eigenvalues of the density matrix throughout the time evolution, as mentioned in the Methods sections. The trace of ρ_S is also checked, as it is required to be unity in every time step.

Another quantity that can be interesting to study is the purity of the system, bound between 1 and the inverse dimension, $\frac{1}{4}$. The purity of ρ_S, alongside its trace, is plotted in Fig. 7. The results show that the system

gets more mixed during the time evolution, always stabilizing close to the lower bound.

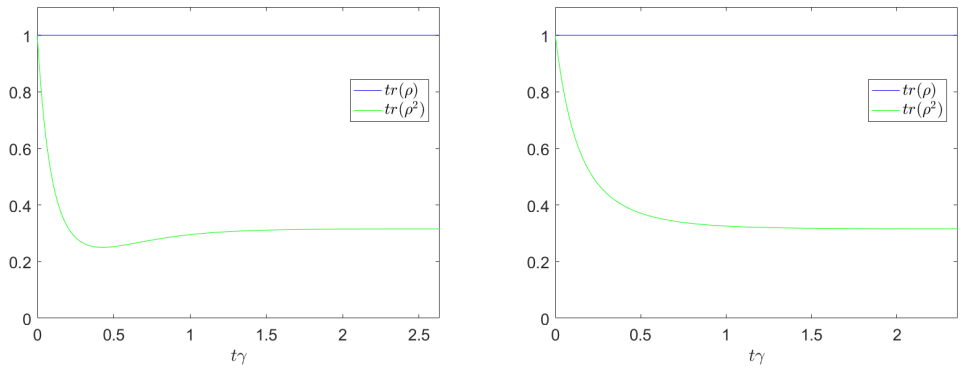

(a) Initial state $|1_c 1_h\rangle$ *(b) Initial state* $|0_c 0_h\rangle$

Figure 7: The figures show the time evolution of the trace and purity of the state of the principal system from two different ancilla states. The remaining parameters used for both simulations are the same as for Fig. 5.

The fact that the purity of the reduced density operator is changing is a confirmation of the openness of the principal system. The purity of a closed quantum system can never change, why Fig. 7 verifies that the qubits are connected to an environment in some way.

4.3 1st and 2nd Laws of Thermodynamics

By plotting Eq. 58, as well as the individual heat currents $\dot{Q}_i$, with respect to time it is possible to get a grasp on the thermodynamic behaviour of the transient regime. Predictions of this behaviour can be made by analysing Fig. 5. When the ground state population decreases all heat currents should reasonably be flowing into the system in order to excite it, thus giving rise to positive $\dot{Q}_i$. Conversely, initial preparation of the system in $|1_c 1_h\rangle$ should result in negative heat currents since energy is released in order to relax the system. These expectations are verified in Fig. 8.

It is clearly seen in Fig. 8 that the system approaches steady state since the sum of the heat currents approaches zero. This behaviour is required by the first law of thermodynamics, which is also used for determining the run time for each simulation. Figure 9 is presented in order to graphically resolve the heat currents close to the steady state regime. The signs of each heat flux appear as expected: heat entering the system from the cold reservoir,

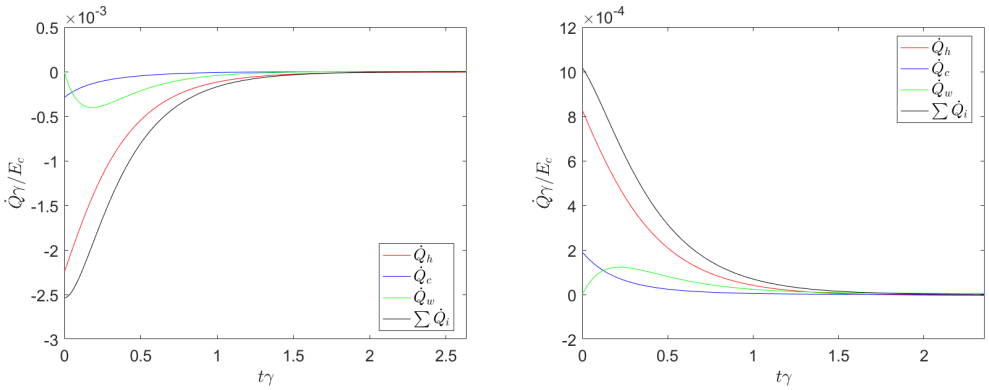

(a) Initial state $|1_c 1_h\rangle$ *(b) Initial state* $|0_c 0_h\rangle$

Figure 8: The figures show the transient heat fluxes, Q_i, from two different ancilla states, as the system approaches steady state. The remaining parameters used for both simulations are the same as for Fig. 5.

$\dot{Q}_c > 0$, and heat leaving the system to the hot reservoir, $\dot{Q}_h < 0$, assisted with additional heat from the work reservoir, $\dot{Q}_w > 0$.

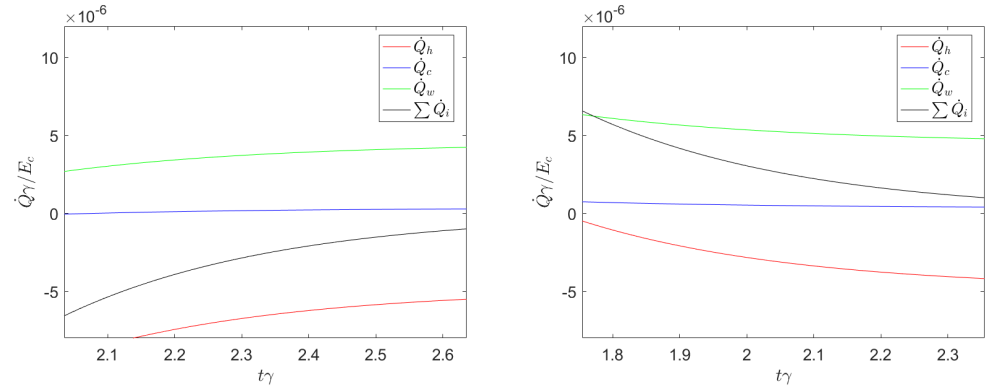

(a) Initial state $|1_c 1_h\rangle$ *(b) Initial state* $|0_c 0_h\rangle$

Figure 9: The figures are zoomed in versions of the data presented in Fig. 8. Here it is possible to resolve the individual heat currents and see that the signs correspond to predictions.

It is now concluded that the initial state of the system will not affect the steady state behaviour of the heat pump. The resulting populations and heat currents will only be a result of the temperatures of the reservoirs, β_i, and the energy splittings of the qubit, E_i. For further results and analysis $|1_c 1_h\rangle$ will be used.

It is also interesting to verify that the system obeys the second law in

terms of entropy production. To study the system's temporal entropy change in the transient regime Eq. 61 is utilized. The entropy change fundamentally has to be a positive quantity in closed systems, in accordance with Fig. 10. Equation 59 is valid in the steady state regime, and it is shown that the entropy change contribution from the reduced system, ΔS_S, declines rapidly. Only the entropy change in the heat reservoirs contribute to the total entropy change in steady state operation.

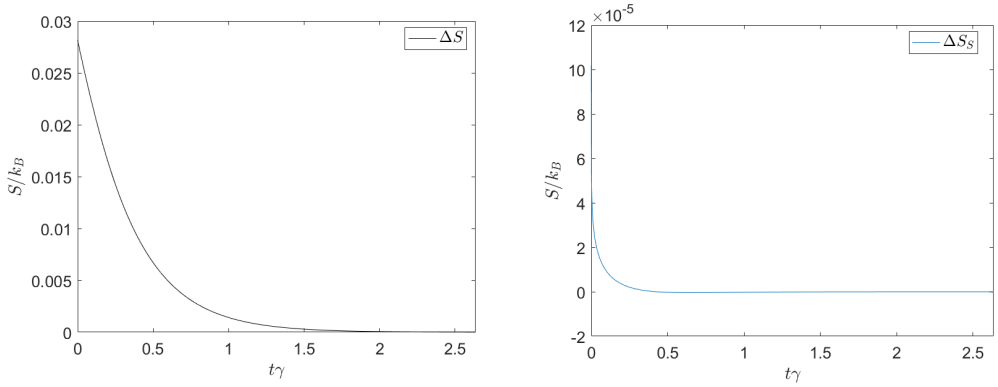

(a) $\Delta S = \frac{dS_S}{dt} - \frac{\dot{Q}_c}{T_c} - \frac{\dot{Q}_h}{T_h} - \frac{\dot{Q}_w}{T_w}$ *(b)* $\frac{dS_S}{dt}$

Figure 10: The figures shows the temporal entropy production in the whole system, ΔS, and the principal system, ΔS_S, respectively. Figure 10a shows that the system behaves according to the second law of thermodynamics. The entropy change of the principal system, ΔS_S is plotted as well in order to show how this quantity quickly approaches 0.

4.4 COP and Cooling Power

The previous results show that the simulation describes a system which over time approaches steady state behaviour. It was also demonstrated that it behaves physically in terms of population distributions, internal energy change and entropy production. The mathematics also seem valid since propagation through the Lindblad equation preserves positivity and unity trace for the density matrix. The change in purity also shows that the principal system is open, i.e. that system-environment interactions are present. At this point the efficiency of the heat pump can be evaluated. This will be done in terms of coefficient of performance and cooling power. The COP for each simulation will be presented as a fraction of the Carnot limit for the specific set up. This is done partly to make the results comparable to each other, partly to see how close the performance is to the theoretical limit. Figure 11 shows a

histogram of the COP, with respect to η_C, achieved from simulations with randomly simulated bath temperatures and qubit energies.

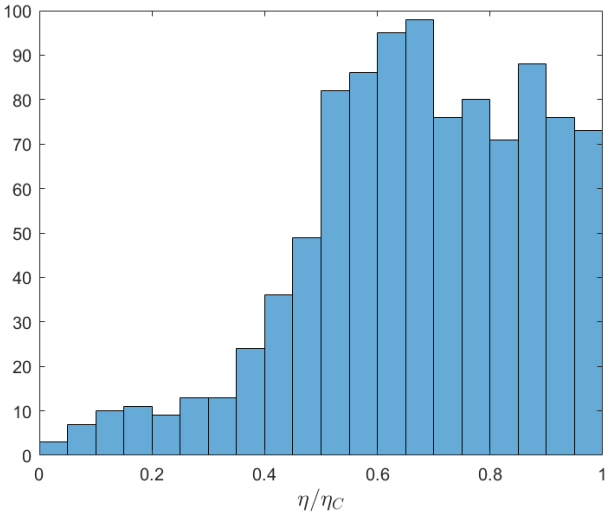

Figure 11: The histogram shows the resulting COP from 1000 simulations with different system parameters. It demonstrates that it is indeed possible to approach the Carnot limit. The highest value achieved was $\eta = 0.992\eta_C$, and 14.9% of the configurations show $\eta > 0.9\eta_C$.

parameter	min	max
γ	0.01	0.01
k_BT_c	$200 \cdot \gamma$	$200 \cdot \gamma$
k_BT_w	k_BT_c	$10 \cdot k_BT_c$
k_BT_h	k_BT_c	k_BT_w
E_h	$\frac{k_BT_c}{2}$	$k_BT_h \cdot 2$
E_c	$\frac{E_c^{max}}{2}$	E_c^{max}
E_w	$E_h - E_c$	$E_h - E_c$

Table 2: The parameters for each simulation were chosen randomly within certain ranges presented in this table. The main constraint is to keep the coupling factor, γ, well below the energies involved in order to respect the weak coupling approximation.

The parameters used for the simulations presented in Fig. 11 are randomly chosen within a large range. Only the ancilla state, $|1_c1_h\rangle$, the coupling factor, γ, and the temperature of the cold bath, T_c, are kept constant. Some

constraints apply to the parameter choices, e.g. the energy scales involved need to be much larger than the coupling factor for the weak coupling approximation to be respected. The parameters are chosen randomly within the ranges presented in table 2.

By comparing the COP and the cooling power in a scatter plot it can be shown that the COP of the heat pump approaches the Carnot limit at the expense of cooling power, and vice versa. Figure 12 shows the COP and Q_c for the same simulations plotted in Fig. 11. A linear fit of the data is included to accentuate the relation between COP and $\dot{Q}_c$.

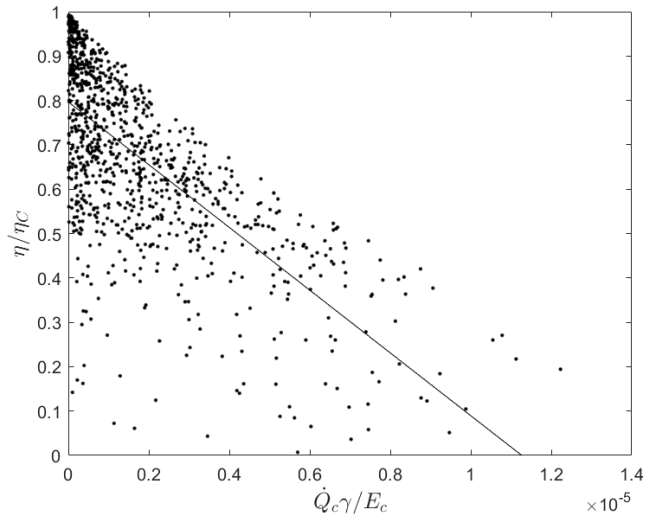

Figure 12: The COP, η/η_C, and the cooling power, $\dot{Q}_c$, of 1000 simulations are plotted in this figure. The figure shows that the Carnot limit, i.e. $\eta/\eta_C = 1$, can be approached only at the expense of cooling power. A linear fit of the data is included to highlight this dependence.

A general dependence of the work reservoir temperature and the energy difference E_w could be found. By reverting to the detailed balance condition, this result is to be expected. This is because the rate ratio $\frac{\Gamma_w^+}{\Gamma_w^-}$ increases for higher T_w, according to Eq. 47. From the same equation it may also be seen that a small E_w has a complementary effect. Thus, by choosing $T_w \gg T_c$ and $E_c \lesssim E_c^{max}$, Fig. 13 is obtained.

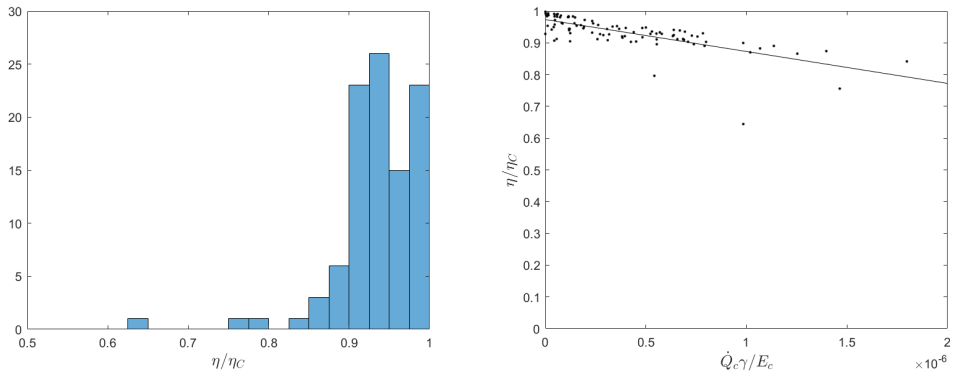

(a) *(b)*

Figure 13: The figures show the results from 100 simulations where $9T_c \leq T_w \leq 10T_c$ *and* $0.9E_c^{max} \leq E_c \leq E_c^{max}$*. The COP is in general closer to the Carnot limit, with 87% of the runs showing* $\eta > 0.9\eta_C$*. Figure 13b also indicates a general improvement in performance.*

The expression for E_c^{max} was analytically derived, but it can be shoved that the limit holds in the simulations as well. If the relation $E_c^{max} < E_c < E_h$ is respected when assigning the parameter values, all heat flows change direction. The cold reservoir is now consequently heated, why the expression for the cooling window holds. An example simulation is presented in Fig. 14.

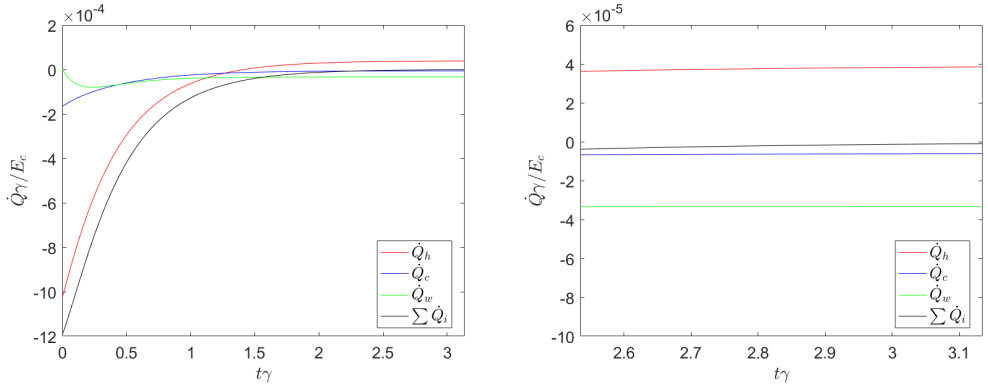

(a) Initial state $|1_c 1_h\rangle$ *(b) Initial state* $|1_c 1_h\rangle$

Figure 14: The figure shows the results from one simulation where $E_c^{max} < E_c < E_h$*. Figure 14a shows the transient behaviour of the heat currents, and Fig. 14b is a zoomed in version of the same plot. From the right plot it can be established that all heat flows are reversed, i.e* $\dot{Q}_h > 0$*,* $\dot{Q}_{c,w} < 0$*.*

5 Summary

Performing a study on quantum thermal machines requires robust understanding of several different fields of physics, e.g. quantum thermodynamics, quantum information theory and dynamics of open quantum systems. Because of this, extensive literature studies had to be undertaken to complete this work. However, this is what makes the field truly exciting. This relatively new branch of physics has been co-developed by scientists from various backgrounds, all carrying different perspectives.

In this thesis it is demonstrated that an absorption driven quantum heat pump could be realized. Particularly, an active medium of only two qubits is studied, with only one additional heat reservoir assisting the process. With a Hilbert space of only 4 dimensions this configuration is one of the smallest thermal machines possible. It is shown that the system acts physically in terms of the models used and that the simulations may approach the fundamental Carnot limit of performance. It is also demonstrated that the performance of the heat pump may be enhanced by choosing the parameters appropriately, in this case T_w and E_w. The analytically derived cooling window, $E_c \leq E_c^{max}$, is finally shown to be valid for simulations as well.

6 Extensions

While this project demonstrates that this configuration of an absorption driven quantum heat pump is theoretically functional, the output could be optimized. It should for example be possible to derive or numerically find the efficiency at maximum cooling power, cf. the Curzon-Ahlborn efficiency of endoreversible thermodynamics.

In [6] the use of non-equilibrium heat reservoirs is investigated. By appropriate tailoring of the heat baths they claim that the Carnot efficiency can be surpassed, thus reaching beyond fundamental classical thermodynamic limits regarding both efficiency and power generation. However, it appears as they have not accounted for the cost of squeezing the reservoirs. This cost should be studied in order to amend this analysis. By considering this cost as a part of the total system, it could possibly be determined if these results still fit into the thermodynamic laws.

There was an initial ambition to study the system from a quantum information perspective as well. Since the time was limited, some of these ideas had to be discarded along the way. The entanglement and decoherence of the system should be studied. By adding a coherent coupling between the qubits this could become more interesting. An idea, for example presented in [8], is to use quantum thermal machines as generators of entanglement. The idea to divert the focus from traditional thermodynamic resources is intriguing and it would present an even more direct connection to the field of quantum information.

Another possibly interesting extension to this project is to get rid of the work reservoir and study a heat pump driven by an external work input. This would perhaps present a more experimentally realizable configuration. Some driving protocol, of e.g. electromagnetic radiation, should exist which makes the set up operate as a heat pump.

7 Appendix

7.1 Operators

As mentioned above, a qubit can be transformed from one state to another. These transformations are governed by a set of, norm preserving, linear operators. In the Bloch sphere representation that means moving the state vector to another point on the surface. This is a good example since it in a simple manner implies the fundamental feature that the norm of a state vector, after any transformation in a closed system, must be preserved (normalization criterion). Thus all allowed operations on a quantum system, called unitary transformations, are any infinitesimal, norm preserving, rotations on the Hilbert space of the specific system.

The books [3] and [15] thoroughly treat the concept of operators, and are used as a foundation for this section. Changes in, or transformations of, physical systems need to be described by the parameter time, t. To unravel how a state evolves with time two general states are assumed: $|\psi\rangle$ at $t = t_0$ and $|\psi\rangle'$ at some $t = t_1 > t_0$. What happens with the state during the conversion from $|\psi\rangle$ to $|\psi'\rangle$? A time evolution operator, $\hat{U}(t_1,t_0)$, is introduced as

$$\begin{gathered} |\psi\rangle \xrightarrow[time\ evolution]{} |\psi'\rangle \\ |\psi'\rangle = \hat{U}(t_1,t_0)\,|\psi\rangle\,. \end{gathered} \tag{86}$$

This operator simply acts on the initial ket to make it $|\psi'\rangle$ after some time interval $t_1 - t_0$. The time evolution operator has to be a unitary operator, i.e. $\hat{U}^\dagger\hat{U} = \hat{U}\hat{U}^\dagger = 1$, in order to satisfy the normalization criterion for the states. The state itself is generally presumed to change with time, which in other words means that the coefficients, $p_a(t)$, of some eigenstates, $|a\rangle$, will change. This can be described mathematically by

$$|\psi(t)\rangle = \sum_a p_a(t)\,|a\rangle \tag{87}$$

However, the sum of the probabilities still has to equal one, in line with

$$\sum_a |p_a(t_0)|^2 = \sum_a |p_a(t_1)|^2 = 1. \tag{88}$$

Given that time is continuous, the time step $t_1 - t_0$ can be chosen arbitrarily small. This leads to the infinitesimal time evolution operator $\hat{U}(t_0+dt,t_0)$.

When this time step dt approaches zero the operator itself must consequently approach identity as

$$\lim_{dt\to 0} \hat{U}(t_0 + dt,t_0) = 1, \tag{89}$$

meaning nothing would happen to the state. All necessary requirements for the infinitesimal time-translation operator are met by expressing it as

$$\hat{U}(t_0 + dt,t_0) = 1 - i\hat{G}dt, \tag{90}$$

with $\hat{G}$ being a Hermitian operator, $\hat{G} = \hat{G}^\dagger$. The operator $\hat{G}$ is actually the Hamilton operator divided by the reduced Planck constant. $\hat{H}$ is system specific and acts as the generator of time translation for this system. The infinitesimal time evolution operator finally takes the form

$$\hat{U}(t_0 + dt,t_0) = 1 - \frac{i\hat{H}dt}{\hbar}. \tag{91}$$

A differential equation for the time evolution operator can be formulated with the ansatz to go from t_0 to $t + dt$ in two steps:

$$\begin{aligned} \hat{U}(t + dt,t_0) &= \hat{U}(t + dt,t)\hat{U}(t,t_0) = \\ &= \left(1 - \frac{i\hat{H}dt}{\hbar}\right)\hat{U}(t,t_0) = \hat{U}(t,t_0) - \frac{i\hat{H}dt}{\hbar}\hat{U}(t,t_0) \end{aligned} \tag{92}$$

and

$$\begin{aligned} \hat{U}(t + dt,t_0) - \hat{U}(t,t_0) &= -\frac{i\hat{H}dt}{\hbar}\hat{U}(t,t_0) \Leftrightarrow \\ \Leftrightarrow \frac{\partial}{\partial t}\hat{U}(t,t_0) &= -\frac{i}{\hbar}\hat{H}\hat{U}(t,t_0). \end{aligned} \tag{93}$$

In the equation above, a state ket, $|\psi(t_0)\rangle$, can be inserted at both sides to obtain

$$\frac{\partial}{\partial t}\hat{U}(t,t_0)\,|\psi(t_0)\rangle = -\frac{i}{\hbar}\hat{H}\hat{U}(t,t_0)\,|\psi(t_0)\rangle\,, \tag{94}$$

and a state at a given time is not time dependent why this is equivalent to

$$\frac{\partial}{\partial t}\,|\psi(t)\rangle = -\frac{i}{\hbar}\hat{H}\,|\psi(t)\rangle\,. \tag{95}$$

This equation is the well known Schrödinger equation (S.E.) for a state vector. It is central to quantum mechanics as it describes the time evolution of a state in any closed quantum system.

The Hamiltonian of a closed and isolated quantum system is time independent. In that case the final expression in Eq. 93 can be integrated to get the time evolution operator on the form of

$$\hat{U}(t,t_0) = \hat{U}(\Delta t) = e^{-\frac{i}{\hbar}\hat{H}\Delta t}. \tag{96}$$

References

[1] Bacon D., *CSE 599d - Quantum Computing One Qubit, Two Qubit*, https://courses.cs.washington.edu/courses/cse599d/06wi/lecturenotes3.pdf, last accessed 28 September 2017.

[2] Brasil C.A., Fanchini F.F., and Napolitano R.d.J., *A simple derivation of the Lindblad equation* https://arxiv.org/pdf/1110.2122.pdf, 2012, last accessed 28 August 2017.

[3] Breuer H.P. and Petruccione F, *The Theory of Open Quantum Systems*, Oxford: Oxford Univ. Press, 2007.

[4] Cappellaro P., *22.51 Quantum Theory of Radiation Interactions* https://ocw.mit.edu/courses/nuclear-engineering/22-51-quantum-theory-of-radiation-interactions-fall-2012/lecture-notes/MIT22_51F12_Notes.pdf, 2012, last accessed 17 January 2018.

[5] Chandra N. and Ghosh R., *Quantum Entanglement in Electron Optics*, Springer, 2013.

[6] Correa, L.A., Palao, J.P., Alonso, D. and Adesso, G., *Quantum-enhanced absorption refrigerators*, https://arxiv.org/pdf/1308.4174.pdf, 2014, last accessed 14 December 2017.

[7] Gamel, O., *Entangled Bloch spheres: Bloch matrix and two-qubit state space*, https://journals.aps.org/pra/pdf/10.1103/PhysRevA.93.062320, 1016, last accessed 14 November 2017.

[8] Goold, J., Huber, M., Riera, A., del Rio, L., and Skrzypczyk, P., *The role of quantum information in thermodynamics — a topical review*, https://arxiv.org/pdf/1505.07835.pdf, 2016, last accessed 2 November 2017.

[9] Hall, B.C., *Quantum Theory for Mathematicians*, New York: Springer, 2013.

[10] Henrich M.J., Mahler G. and Michel M., *Driven spin systems as quantum thermodynamic machines: Fundamental limits*, https://journals.aps.org/pre/pdf/10.1103/PhysRevE.75.051118, 2007, last accessed 13 October 2017.

[11] Lawrence, W.E., *Detailed balance, quantum distribution functions, and equilibrium of mixtures*, American Journal of Physics, Volume

67, Issue 12, http://aapt.scitation.org/doi/pdf/10.1119/1.19097, 1999, last accessed 23 January 2018.

[12] Lindblad, G., *On the Generators of Quantum Dynamical Semigroups*, Commun. math. Phys. 48, 119—130, Springer, Springer, 1976, arxiv.org/abs/quant-ph/0606228, 2006, last accessed 16 January 2018.

[13] Nielsen, M.A. and Chuang, I.L. *Quantum Computation and Quantum Information*, Cambridge: Cambridge University Press, 2003.

[14] Palao, J.p. and Koslof, R., *Quantum thermodynamic cooling cycle*, https://arxiv.org/pdf/quant-ph/0106048.pdf, 2001, last accessed 6 February 2018.

[15] Sakurai, J.J. and Napolitano, J. *Modern Quantum Mechanics*, 2nd edn., San Fransisco: Pearson Education Inc., 2011. y

[16] Scovil H.E.D. and Schulz-DuBois E.O., *Three-level masers as heat engines*, https://journals.aps.org/prl/pdf/10.1103/PhysRevLett.2.262, 1959, last accessed 26 January 2018.

[17] Vinjanampathy, S., Anders, J., *Quantum Thermodynamics*, https://arxiv.org/pdf/1508.06099.pdf, 2016, last accessed 18 December 2017.